

Transport of spatial quantum correlations through an optical waveguide

J. Hordell,¹ D. Benedicto-Orenes,¹ P. G. Petrov,^{1,*} A. U. Kowalczyk,¹ G. Barontini,¹ and V. Boyer^{1,†}

¹*Midlands Ultracold Atom Research Centre, School of Physics and Astronomy,
University of Birmingham, Edgbaston, Birmingham B15 2TT, UK*

The ubiquity of optical communications is due in large part to the advent of the optical fibre, which allows for flexible and efficient routing of light-encoded information. Used as serial channels, single fibres have also been shown to be effective to transport quantum information, for instance in commercial quantum key distribution systems [1]. As fibre technology progresses to support the transmission of full images, e.g. in endoscopic devices, the question arises whether this technology is also suitable for the parallel transport of spatial quantum information, such as quantum images [2]. Here we demonstrate the transport of quantum intensity correlations through a conduit made of the ordered packing of thousands of fibres, in a way which preserves localised intensity-difference squeezing. Maintaining the spatial character of quantum information opens the way to the use of guided-light technology in the emergent field of quantum imaging.

Optical fibre bundles are readily used to transport information in the form of classical images, for example in endoscopy devices [3]. In these applications, the information is contained in the local amplitude of the light field incident on the input face of the bundle. The ordered packing of the fibres in the bundle guarantees the conservation of the light intensity distribution across the beam profile, therefore the image is preserved during the propagation and reappears on the output face of the bundle. The question remains whether one can extend this property to the quantum domain. This will be equivalent to ensuring that the quantum correlations associated with the intensity fluctuations of an arbitrary spatial feature, that is to say an input transverse mode, are reproduced on the output of the guide in the exact same mode.

Previous experimental research in the guiding of the spatial quantum states of light has been essentially limited to the single-photon subspace. For instance, the guided transport of photons spatially entangled over two modes has been demonstrated in a Kagome fibre [4]. Beyond a small number of modes, only the spatially-resolved detection of photons has been demonstrated, typically by combining a fibre bundle to an ensemble of single-photon detectors. In this manner, the temporal nonclassical statistics of spatially resolved photons emitted by scattered emitters was observed over a bundle of 15 fibres [5]. Such spatially resolved guiding of single photons, or photons belonging to correlated pairs, could be useful to channel illumination or signal in low-light-level quantum imaging applications [6]. The interest in transporting quantum states of light for imaging however, goes beyond these low fluxes of photons. Macroscopic states of light are better suited to the imaging of hard-to-see objects, e.g. very weakly absorbing objects, because at the quantum noise limit (QNL) a larger probing intensity provides a better signal-to-noise ratio. In this context, bright two-mode squeezed states of light, containing arbitrary mean numbers of photons, have been

shown to display local intensity correlations below the shot noise limit both in the frequency [2] and time domains [7], and are therefore good candidates for practical quantum imaging. This is particularly true for those applications where the illumination intensity cannot be arbitrarily increased due to the existence of a damage threshold [8], and where squeezing the quantum fluctuations of light are the only solution to increase the signal to noise ratio.

Here we address the issue of the transport of a bright illumination with a fibre bundle while preserving local intensity fluctuations at the quantum level. Starting from a two-mode squeezed state [9], that is to say a pair of continuous-variable (CV) entangled light beams which display intensity and phase quantum correlations of their random spatial fluctuations, we transport one of the beams through the bundle and show that the spatial intensity correlations with the other beam are preserved, as evidenced by the presence of local intensity-difference squeezing after the transport.

The two-mode squeezed state is created using a phase-insensitive optical amplifier. Our amplifier is based on four-wave-mixing (4WM) in a hot ⁸⁵Rb vapour in a double-lambda configuration [10], as described in the Methods section. The process is efficient enough to realise a nonlinear single-pass gain of a few units without the need of an enhancement cavity. This travelling-wave amplifier, because it has a gain region of finite length, does not enforce a strict phase-matching condition and the resulting two-mode squeezed state is intrinsically spatially multimode. This means that the twin beams, probe and conjugate, are entangled across multiple spatial modes, or regions [2]. In particular, matching pairs of locales in the cross-sections of the beams are correlated. In the plane of the cell, referred to as the near field, these regions are mapped onto each other because probe and conjugate correlated fluctuations are born in the same location. In the far field these regions are symmetrically placed about the pump propagation axis due to transverse momentum conservation. Diffraction associated with the propagation over the finite length of the cell leads to a minimum transverse size over which corre-

* p.g.petrov@bham.ac.uk

† v.boyer@bham.ac.uk

lations can be observed, the coherence area [11], with an associate coherence length [?]. As the coherence area is substantially smaller than the beams size, a large number of modes, typically a few tens, are independently correlated. This unique feature makes the twin beams a useful resource for imaging with sensitivity [12] or resolution [13] beyond the shot-noise limit, and efficiently guiding of the beams would make these applications more practical.

We chose to focus on intensity correlations in the near field. To this effect, we separate the twin beams and we image their nonlinear interaction region onto individual “measurement” planes, as shown in Fig.1. In these planes, identical locations on the twin beams display quantum intensity correlations which we aim to preserve after transport in a fibre bundle.

The fibre bundle itself is a rigid conduit, designed to transmit (coherently) optical images with a resolution given by the fibre size. It is 15cm long and contains 5×10^4 fibres with diameter of $12\mu\text{m}$ tightly packed into a equilateral triangular lattice. Fig. 2(a) shows an image of the output face of the conduit injected with a Gaussian beam of diameter smaller than the conduit diameter, and reveals the packing structure. The incomplete filling leads to an overall transmission of around 30%, primarily determined by the ratio of the fibre core total area to the conduit input face area, but also by partial reflection on the faces of the conduit. The large core size of the fibres makes them multimode for near-infrared optical wavelengths, as evidenced by the irregularity in the shapes of the light beams coming out of the individual fibres.

The discretisation introduced by the finite fibre size sets a natural length scale for the smaller spatial details that can be transmitted by the conduit. At the quantum level, one can expect that only fluctuations of spatial modes substantially larger than the inter-fibre spacing will be accurately transmitted across the guide. We therefore image the beam on the input face of the conduit in such a way that the fibre size is much smaller than the estimated coherence area, as shown in Fig.2(a). This means that all the scales of correlations present in the system should be successfully transmitted.

The loss of probe light due to the finite transmission of the conduit induces a mismatch between the probe and conjugate fluctuations at the balanced photodetector, which can be corrected by introducing an adequate level of attenuation on the conjugate beam, as shown in Fig. 1. Since the effect of loss on a beam of light is to mix vacuum noise to the fluctuations of the beam, the measured squeezing after loss is less than the squeezing before loss. Therefore the initial degree of squeezing (3.0 dB) and the level of attenuation of the conjugate (25%) are chosen to maximise the level of squeezing seen after the conduit. The details of the procedure are given in the Supplementary Information.

Although the fibre bundle conserves the coarse distribution of intensity between the input and the output, modal dispersion, i.e. group velocity dispersion for different spatial modes within each fibre [14] as well as differen-

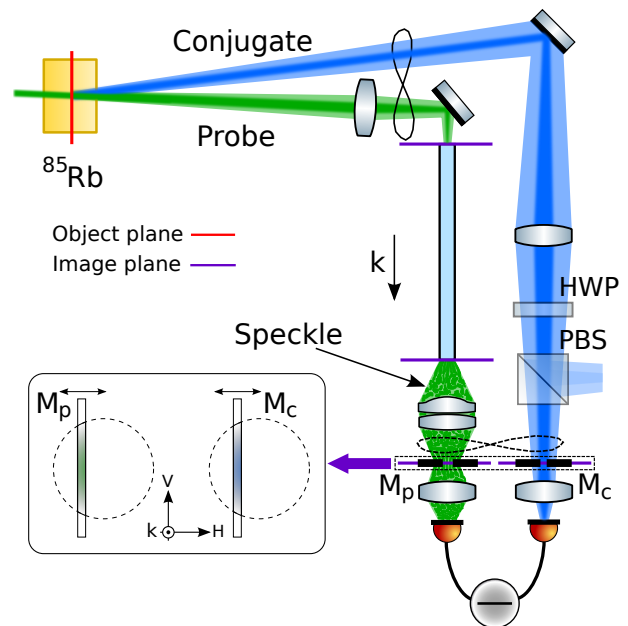


FIG. 1. **Experimental setup.** The conjugate and probe beams are generated via 4WM in the ^{85}Rb cell. The probe light in the object plane, i.e. the plane at the position of the cell, where the correlations are created, is imaged onto the input face of the conduit. The probe light emerging from the output face of the conduit is imaged onto the probe slit on the measurement plane (M_p) using a high numerical aperture optical system. The conjugate is directly imaged onto the conjugate slit on the measurement plane (M_c). The conjugate slit is translated in horizontal (H) and vertical (V) directions perpendicular to the direction of propagation k , for every position of the probe slit as shown in the inset. The polarising beamsplitter (PBS) and the half-wave plate (HWP) in the path of the conjugate provide a tunable loss for the channel to balance the beams intensities in the case where the probe is sent through the conduit. The lightly coloured paths depict the geometric propagation of the quantum fluctuations whereas the densely coloured paths depict the Gaussian propagation of the bright probe and conjugate beams. The pump beam is not shown for clarity. The figures of eight indicate CV entanglement (solid line) and quantum intensity correlations (dashed line).

tial dispersion between the fibres, leads to the scrambling of the phase of the output field on a length scale of the order of the size of the fibre cores. As a consequence of this wavefront distortion, the output beam is diffracted following a large numerical aperture (0.55) and produces in the far field the speckle pattern shown in Fig.2(b). Since the spatial correspondence of the intensity between the input and output faces does not extend to regions away from the faces, faithful transmission of the intensity fluctuations puts stringent requirements on the accuracy of the imaging of the plane of interest onto the input face of the conduit. Similarly, the output plane has to be accurately imaged onto the measurement plane. Because of the strong diffraction, the collection optics requires a high numerical aperture (0.5) and has to be accurately

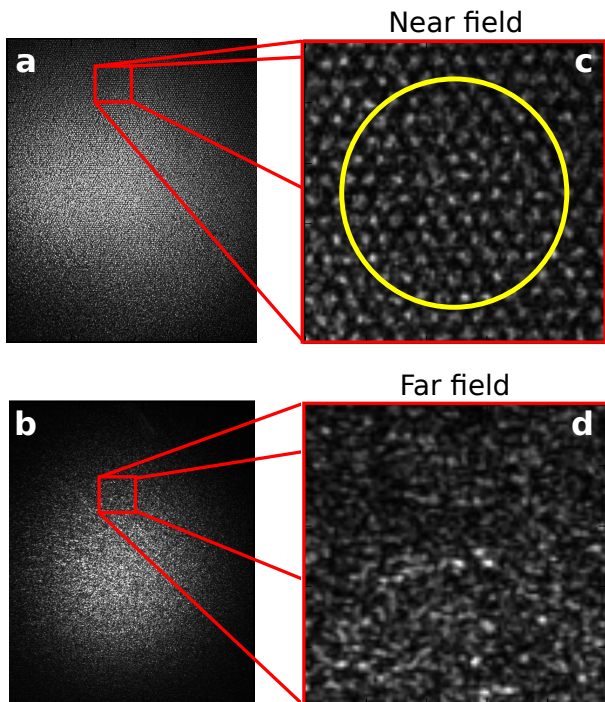


FIG. 2. **Images of the probe beam after the conduit.** **a,b** Images of the near- and far-field beam patterns after the conduit, showing the Gaussian intensity envelope. **c,d** Selected magnified regions across the profiles in **a** and **b**, respectively. In **c**, in the near-field, the characteristic pattern coming from the hexagonal lattice of constituent fibres can be clearly seen at the output face of the conduit. The lattice spacing is about $12 \mu\text{m}$. Since the fibres are multimode, the emerging mode shape is random across the fibre lattice. The enclosed circular area represents the estimated coherence area of the process. In **d**, in the far field the fibre lattice pattern is transformed into a speckle pattern as the light from every fibre acquires a random phase.

placed due to the resulting very short depth of field.

In practice, we test the spatial correlations by selecting small regions on the measurement planes with two movable slits, one on the probe beam and one on the conjugate beam (Fig. 1). The partial powers transmitted through the slits are detected by the separate photodiodes of a balanced photodetector which forms the subtraction of the photocurrents. The noise of the photocurrent difference is measured with a spectrum analyser, and recording the intensity-difference noise as a function of the position of the slits allows us to map the spatial intensity correlations between probe and conjugate. Selecting correlated regions leads to reduced noise below the QNL, whereas mismatched positions produce excess noise associated with phase-insensitive optical amplification. We perform the experiment twice. Firstly, we characterise the spatial correlations generated by the 4WM alone. Secondly, we measure the same spatial correlations after sending the probe beam through the conduit, as shown in Fig.1.

The slits are set up on pair of translation stages and their width is set to be of the order of the coherence length. While it is possible to accurately evaluate the coherence length [15], we adopt here a more straightforward methodology which consists in selecting widths of the slits which cause a significant reduction of measured squeezing. Reducing the slits sizes increases the share of the spatial frequency spectra of the transmission functions of the slits which lie outside the spatial bandwidth of the 4WM process and corresponds to transmitted modes in a vacuum state. If this fraction of the spectrum dominates, the measured noise will tend to the QNL. Note that the spatial spectra associated with the gate-shaped transmission function of the slits always contain high spatial frequencies that lie outside the 4WM spatial bandwidth, which is given by the coherence length. It is therefore expected that selecting correlated regions with slits will always generate reduced measured squeezing. Experimentally the slits are set to $\approx 15\%$ of the beams widths and provide an overestimate of the coherence length [16], theoretically estimated to be around $120 \mu\text{m}$ which is about 8% of the beams size. After the width is selected, the slits are scanned across the span of the beams, scanning over the conjugate for each region across the probe. Fig.3 shows the noise recorded by the balanced detector for each pair of positions of the slits. A reduction in the intensity-difference noise below the QNL over a background of excess noise is observed when the slits positions match, that is to say they are identical inside the probe and conjugate beams.

Comparing the data with and without the bundle, it is apparent that, apart from a reduction of the overall level of squeezing due to the finite transmission of the device, the conduit preserves the spatial properties of the quantum state of the light, here the intensity quantum fluctuations. As expected, the spatial resolution of the conduit is better than the coherence length of the beam profile. Indeed the fibre size is 10 times smaller than the coherence length of the transmitted quantum field, which, as estimated by the width of the narrowest trough in Fig.3(d) is of the order of $100 \mu\text{m}$. The exact shape of the noise dips is the result of a combination of the slits transfer function and the coherence profile. The width of the dips can therefore be used to estimate trends of the relative size of the coherence area with respect to the beam sizes. For a fixed slit width, a wider noise dip implies a larger coherence length. In order to gauge the effect of the conduit on the spatial frequency bandwidth of the correlations, we consider the width of the squeezing troughs, κ , relative to the Gaussian beam diameter. In the case of transmission through the conduit, κ is found to be 0.32 and 0.29, for horizontal and vertical scans respectively. In the case of free space propagation, κ is 0.27 and 0.20, respectively.

The comparison between the values of κ with and without the conduit shows that the spatial bandwidth of the spatial correlations is largely preserved during transport. The small loss of spatial resolution can be attributed to a

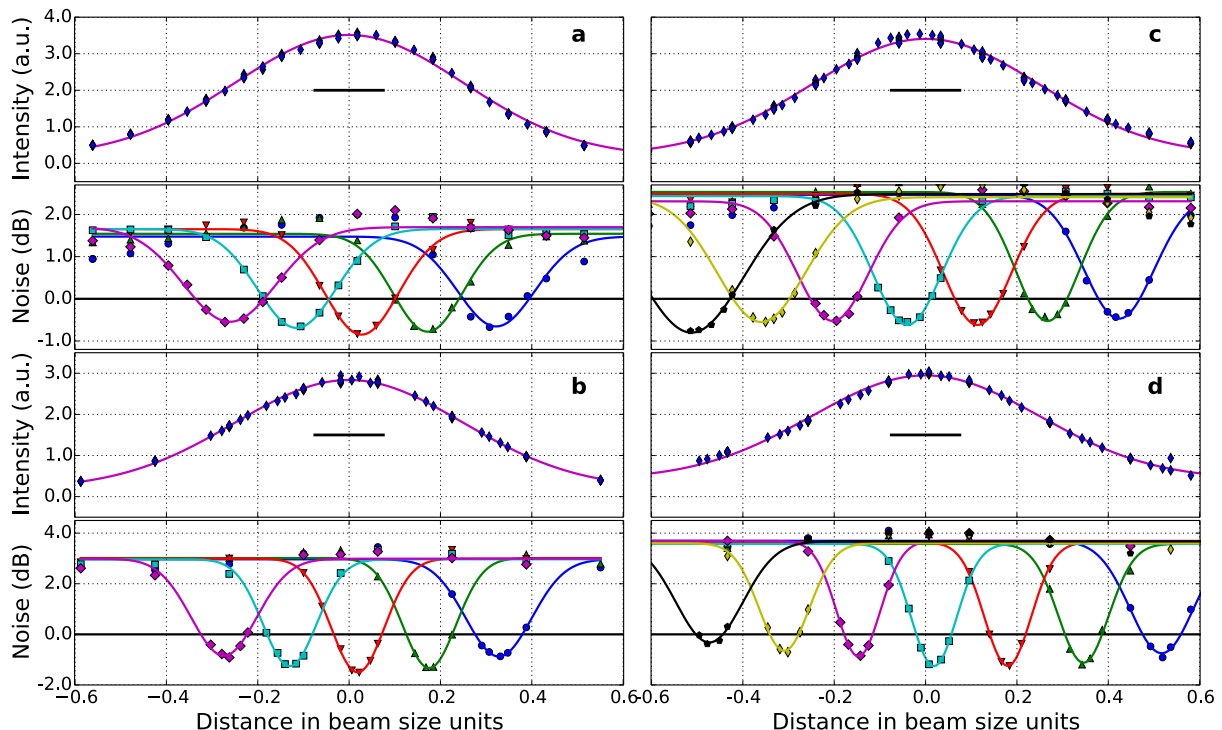


FIG. 3. **Scanning noise data relative to shot noise.** The measurement procedure is done by scanning the slit position on the conjugate beam for fixed positions of the slit on the probe beam. The result is a single dip in the detected noise for each scan. The scanning is done in both horizontal **a,b** and vertical **c,d** directions for the cases where the conduit is inserted in the probe beam path in **a,c**, and when it is not present **b,d**. The top graph in each figure is the fitted intensity profile of the conjugate beam. The noise dips are fitted using Gaussians and the black solid line at 0 dB represents the shot noise. The bar in each beam profile graph denotes the slit size. The excess amplification noise, observed when the slits positions do not match, is larger at the centre of the gain medium, where the Gaussian pump beam profile peaks and the gain is the largest. The intensity profile of the conjugate beam is given in arbitrary units (a.u.).

combination of imperfections in the imaging system and conduit behaviour. Firstly, the very small depth of field of the high-numerical aperture imaging system, which is required to efficiently collect the light after the conduit, could result in an approximate imaging of the output face of the conduit on the slit. This works in combination with the spherical aberrations of the optical system. Secondly, the conduit itself has a small but not negligible cross-talk between fibres [17], which leads to the smearing of the correlations over adjacent correlated regions, resulting in larger width of the troughs.

The two-mode squeezed state generated by the 4WM process nominally displays phase-sum squeezing which, together with the intensity-difference squeezing, results in continuous-variable entanglement [18, 19]. Phase scrambling by the conduit prevents us from directly measuring phase correlations, however phase randomisation due to modal dispersion is to be understood with respect to an external reference. Indeed, phase information can still be transmitted as long as a bright coherent carrier is also transmitted so as to serve as a local phase reference, as it is done in this experiment by using a bright beam. The beam emerging from the conduit should display phase fluctuations locally correlated with the phase

fluctuations of the other twin beam. Measuring such correlations would require a local oscillator with a wavefront which matches the wavefront of the light on the output face of the conduit. Phase control of the local oscillator with a spatial resolution better than the fibre array resolution would be a formidable yet feasible task.

Another solution to the issue of wavefront distortion is direct control of modal dispersion, so that the transmitted beam emerges from the conduit with a flat wavefront. Simply using single-mode fibres as the constituents of the bundle can avoid modal dispersion within individual fibres, but controlling or correcting for the differential dispersion between the fibres is much harder. Nonetheless there has been progress in real time compensation of modal dispersion to perform classical imaging through single multimode guides or fibres [20–22]. Improving substantially on the spatial resolution of these techniques may lead to the possibility of guiding and preserving the full quantum state of the electromagnetic field, thereby extending the work of Ref. [4] to larger numbers of spatial modes and arbitrary photon numbers.

In conclusion, we have demonstrated that spatial quantum intensity correlations, in the form of localised intensity-difference squeezing, can be transported

through a fibre bundle. Our work provides initial step towards the realisation of practical quantum enhancement in imaging applications where the shot noise is a limitation and where light guiding provides additional convenience. Our experiment uses a standard commercially available conduit, however improved performance could be obtained with a purpose-build device made of single mode fibres for a reduced distortion of the wavefront, more fibres for improved spatial resolution, and optimised packing for increased transmission. Additionally, realising active phase control would extend the method presented here to the effective guiding of massively parallel entanglement, with possible use in parallel quantum communication links.

METHODS

Four-wave-mixing. The quantum correlations are generated using a non-degenerate 4WM process in a hot ^{85}Rb atomic vapour in a double-lambda configuration [10]. A strong 795 nm pump beam (700 mW) and a weak seed beam (130 μW) intersect at a small angle of ~ 6 mrad into a 12 mm-long vapour cell heated to $\gtrsim 100^\circ\text{C}$. The probe beam is derived from the pump beam via an AOM in a double-pass configuration driven at a frequency of 1.5 GHz, half the ground state hyperfine splitting. The pump and the probe are resonant with a two-photon Raman transition between the hyperfine ground states, with a detuning of ~ 800 MHz to the blue of the $F = 2 \rightarrow F'$ and $F = 3 \rightarrow F'$ transitions, respectively.

The 4WM process corresponds to the transfer of an atom from the $F = 3$ hyperfine ground state to the $F = 2$ hyperfine ground state and back to the initial state. In the process the atom consumes two pump photons and emits one probe photon as well as one conjugate photon at a frequency ~ 6 GHz higher than the probe frequency and located symmetrically with respect to the pump beam axis [10]. The hot atomic vapour acts as a phase-insensitive amplifier for the probe with a single-pass gain of 1.5-2. This is enough to amplify the probe and generate a conjugate beam in a travelling-wave configuration, that is to say without the use of a cavity. The bandwidth of the nonlinear process is about 20 MHz.

Optical imaging. To reveal the intensity spatial correlations produced locally in the gain medium, the median plane in the vapour cell, the near field, must be imaged on the selection slits. When the conduit is introduced in the probe path, the near field must in addition be imaged on the input facet of the conduit. Direct imaging of the near field on the conduit or the slits is done with a single long-focal-length lens of 250 mm. Imaging of the exit facet of the conduit on the probe selection slit is done with high-numerical-aperture doublet made of 8 mm focal length aspheric lens and a 16 mm focal length lens.

Noise detection. The light going through the slits is detected by a balanced photodetector with quantum efficiency of 95%. For practical reasons, the gain is identical for both photodiodes. The trans-amplified differential photocurrent is analysed with a spectrum analyser operating at an analysing frequency of 2 MHz, a resolution bandwidth of 30kHz, and a video bandwidth of 30Hz.

-
- [1] M. Peev et al., “The SECOQC quantum key distribution network in Vienna,” *New. J. Phys.*, **11**, 075001 (2009).
 - [2] V. Boyer, A. M. Marino, and P. D. Lett, “Generation of spatially broadband twin beams for quantum imaging,” *Phys. Rev. Lett.*, **100**, 143601 (2008).
 - [3] Venkataraman Subramanian and Krish Raguath, “Advanced endoscopic imaging: A review of commercially available technologies,” *Clinical Gastroenterology and Hepatology*, **12**, 368 – 376.e1 (2014).
 - [4] W. Löffler, T. G. Euser, E. R. Eliel, M. Scharrer, P. St. J. Russell, and J. P. Woerdman, “Fiber transport of spatially entangled photons,” *Phys. Rev. Lett.*, **106**, 240505 (2011).
 - [5] Yonatan Israel, Ron Tenne, Dan Oron, and Yaron Silberberg, “Quantum correlation enhanced super-resolution localization microscopy enabled by a fibre bundle camera,” *Nature Communications*, **8**, 14786 (2017).
 - [6] G. Brida, M. Genovese, and I. Ruo-Berchera, “Experimental realization of sub-shot-noise quantum imaging,” *Nat. Photon.*, **4**, 227–230 (2010).
 - [7] Ashok Kumar, Hayden Nunley, and A. M. Marino, “Observation of spatial quantum correlations in the macroscopic regime,” *Phys. Rev. A*, **95**, 053849 (2017).
 - [8] M. A. Taylor, J. Janousek, V. Daria, J. Knittel, B. Hage, H.-A. Bachor, and W. P. Bowen, “Experimental realization of sub-shot-noise quantum imaging,” *Nat. Photon.*, **7**, 229–233 (2013).
 - [9] A. Heidmann, R. J. Horowicz, S. Reynaud, E. Giacobino, C. Fabre, and G. Camy, “Observation of quantum noise reduction on twin laser beams,” *Phys. Rev. Lett.*, **59**, 2555–2557 (1987).
 - [10] C. F. McCormick, V. Boyer, E. Arimondo, and P. D. Lett, “Strong relative intensity squeezing by four-wave mixing in rubidium vapor,” *Opt. Lett.*, **32**, 178–180 (2007).
 - [11] E. Brambilla, A. Gatti, M. Bache, and L. A. Lugiato, “Simultaneous near-field and far-field spatial quantum correlations in the high-gain regime of parametric down-conversion,” *Phys. Rev. A*, **69**, 023802 (2004).
 - [12] E. D. Lopaeva, I. Ruo Berchera, I. P. Degiovanni, S. Olivares, G. Brida, and M. Genovese, “Experimental realization of quantum illumination,” *Phys. Rev. Lett.*, **110**, 153603 (2013).
 - [13] Michael A. Taylor, Jiri Janousek, Vincent Daria, Joachim Knittel, Boris Hage, Hans-A. Bachor, and Warwick P. Bowen, “Subdiffraction-limited quantum imaging within a living cell,” *Phys. Rev. X*, **4**, 011017 (2014).
 - [14] A. Yariv, *Optical Electronics* (Saunders College Publish-

- ing, 1991).
- [15] M. W. Holtfrerich and A. M. Marino, “Control of the size of the coherence area in entangled twin beams,” *Phys. Rev. A*, **93**, 063821 (2016).
 - [16] C. S. Embrey, M. T. Turnbull, P. G. Petrov, and V. Boyer, “Observation of localized multi-spatial-mode quadrature squeezing,” *Phys. Rev. X*, **5**, 031004 (2015).
 - [17] A. Perperidis, H. E. Parker, A. Karam-Eldaly, Y. Altmann, K. Dhaliwal, R. R. Thomson, M. G. Tanner, and S. McLaughlin, “Characterization and modelling of inter-core coupling in coherent fiber bundles,” *Opt. Express*, **25**, 11932–11953 (2017).
 - [18] V. Boyer, A. M. Marino, R. C. Pooser, and P. D. Lett, “Entangled images from four-wave mixing,” *Science*, **321**, 544 – 547 (2008).
 - [19] M. D. Reid, “Demonstration of the einstein-podolsky-rosen paradox using nondegenerate parametric amplification,” *Phys. Rev. A*, **40**, 913–923 (1989).
 - [20] Amir Porat, Esben Ravn Andresen, Hervé Rigneault, Dan Oron, Sylvain Gigan, and Ori Katz, “Widefield lensless imaging through a fiber bundle via speckle correlations,” *Opt. Express*, **24**, 16835–16855 (2016).
 - [21] Alexander Fertman and Dvir Yelin, “Image transmission through an optical fiber using real-time modal phase restoration,” *J. Opt. Soc. Am. B*, **30**, 149–157 (2013).
 - [22] Tomas Cizmar and Kishan Dholakia, “Exploiting multi-mode waveguides for pure fibre-based imaging,” *Nature Communications*, **3**, 1027 (2012).

ACKNOWLEDGEMENTS

The authors acknowledge support from the Engineering and Physical Sciences Research Council, Grants No.

EP/I001743/1 and No. EP/M013294/1. J. H. was supported by the Defence Science and Technology Laboratory research PhD program via contract No. DSTL-1000092268.

AUTHOR CONTRIBUTIONS

J.H., D.B. and A.K. constructed the apparatus, J.H. took the data, P.G.P. analysed the data and wrote the article with the help of V.B. The principal investigators V.B. and G.B. designed the experiment and provided guidance. All authors commented on the manuscript, discussed its structure, data analysis and interpretation.

ADDITIONAL INFORMATION

Supplementary information is provided. The authors declare no competing financial interests. Reprints and permission information is available online at www.nature.com/reprints. Correspondence and requests for materials should be addressed to P.G.P. and V.B.